High domain wall velocities in in-plane magnetized (Ga,Mn)(As,P) layers

L. Thevenard, Syed Asad Hussain, Hans Jürgen von Bardeleben, Mathieu Bernard, A Lemaitre, C. Gourdon

High domain wall velocities in in-plane magnetized (Ga,Mn)(As,P) layers

L. Thevenard[1], S. A. Hussain[1], H. J. von Bardeleben[1], M. Bernard[1], A. Lemaître[2] , C. Gourdon[1]
[1] *Institut des Nanosciences de Paris, Université Pierre et Marie Curie, CNRS, UMR7588, 4 place Jussieu,75252 Paris, France*
[2] *Laboratoire de Photonique et Nanostructures, CNRS, UPR 20, Route de Nozay, Marcoussis, 91460, France*

(Dated: February 7, 2012)

Field-induced domain wall (DW) propagation was evidenced in unpatterned layers of in-plane magnetized $Ga_{1-x}Mn_xAs_{1-y}P_y$ using Kerr microscopy. Both stationary and precessional regimes were observed, and domain wall velocities of up to 500 m s^{-1} were measured, of the order of magnitude of those observed on in-plane magnetized metals. Taking advantage of the strain-dependent magneto-crystalline anisotropy in this dilute magnetic semiconductor, both out-of-plane and in-plane anisotropies were adjusted by varying the manganese and phosphorus concentrations. We demonstrate that these anisotropies are a critical parameter to obtain large velocities. These results are interpreted in the framework of the one-dimensional model for domain wall propagation.

PACS numbers: 75.50.Pp,75.60.Ch,75.78.Fg

Spintronics has spurred a renewed interest in in-plane magnetized materials, with soft ferromagnets being used in novel shift-register memories based on magnetic domain wall propagation (DWP)[1,2]. To be viable, these devices require an excellent knowledge of the physics governing the DW velocity and structure, via the micromagnetic parameters of the material. Among them, the magnetic anisotropy - shape or magneto-crystalline - governs the canting of the magnetization within the domain wall, which propels it forward[3]. Nanostructuring the devices was thus a substantial progress as it induces shape anisotropy[4,5] and somewhat simplifies the theoretical treatment of the problem[3]. However, confinement also introduces edge roughness that is complex to model, and imposes a sample design for a desired DW velocity behavior (such as the maximum velocity, or the maximum field giving a stationary configuration of the DW). Past experiments have studied at length the effects of shape anisotropy on the DW velocity in metals[4,5], but no exploration has been done of the powerful lever that is magneto-crystalline anisotropy. This was mostly due to the difficulty to tune it over a broad range in metals, and to the technical issues linked to measuring high DW velocities at fields higher than a few Oersteds[6].

In this context, we believe dilute magnetic semiconductors (DMS) to be ideally suited materials for these studies. In particular the model material GaMnAs, and its Phosphorus substituted compound offer obvious advantages: micromagnetic parameters that can be tuned during[7] or after the growth[8], and weak DW pinning permitting the observation of intrinsic flow regimes for field-driven DW propagation in out-of-plane magnetized layers[9]. DWP studies on in-plane magnetized GaMnAs layers have been limited to observations of the magnetic after-effect in the creep regime[10], and transport measurements of low DW velocities in micron-wide stripes[11]. In this geometry, the interplay between magnetic anisotropies and DWP could not be studied. Working on unpatterned layers and tuning the magnetic anisotropies in GaMnAs(P) alloys would however provide unprecedented understanding and control of the field dependence of the velocity. Moreover these layers should be well suited to achieve high DW velocities because of large DW width[12], as expected from the well-known one-dimensional (1D) model[13,14] for DW propagation.

In this model, the field-induced propagation is expected to consist of a stationary linear regime, followed beyond the Walker field H_W by a precessional regime. An interesting case occurs when samples exhibit both a strong perpendicular uniaxial magnetic anisotropy making the sample plane an easy plane (coefficient $K_\perp$) and a uniaxial in-plane anisotropy (coefficient K_0). In this configuration, the Walker field is expected to depend solely on $K_\perp$ and the DW width on K_0. However, the maximum velocity in the stationary regime depends on the relative weight of both anisotropies[3].

In this Letter, we evidence using longitudinal Kerr microscopy the propagation of DWs in the flow regimes, both stationary and precessional, in GaMnAs(P) layers with in-plane magnetization. DW velocities comparable to those found in Permalloy (Py), and over ten-fold higher (up to 500 m s^{-1}) than any recorded speeds in DMS are measured. Several samples are investigated to understand the impact of the different magnetic anisotropies on the DW dynamics, in particular on the maximum achievable velocities.

Four 50 nm thick $(Ga_{1-x}Mn_x)(As_{1-y}P_y)$ samples were studied. Their characteristics are given in Table I and Ref. 15. The magnetic anisotropy coefficients $K_{2\perp}$, $K_{4\perp}$, $K_{2//}$, $K_{4//}$ are determined by ferromagnetic resonance (FMR) (see Ref. 16 for details). They can equivalently[16] be expressed in terms of an effective out-

sample	$[Mn]_{eff}$ (%)	T_C (K)	[P] (%)	lm (ppm)	T (K)	$K_\perp$ (J m^{-3})	K_0 (J m^{-3})	V_{max} from Eq. (1) (m s^{-1})	v_{max} measured (m s^{-1})	$\mu_0 H_{max}$ measured (mT)
A4	4.7	130	0	6890 ±30	**25**	**10120**	**486**	**335**	**507**±23	**7.8**
					60	7481	366	356	492±16	5.1
					85	4781	58	412	481±28	3.6
A3	3.7	122	0	4990 ±80	**20**	**7415**	**40**	**239**	**328**±29/**403**±35	**5.4/7.6**
					60	4626	117	240	292±12	2.5
B3	3.7	134	2.6	280 ±150	**20**	**3461**	**19**	**163**	**186**±16	**3.2**
					60	2370	54	155	142±9	2.7
C3	3.7	110	3.4	0 ±400	**30**	**2039**	**62**	**101**	**100**±7	**2.6**
					60	1454	32	122	100±3	2.6

TABLE I. Main characteristics of the samples[15], with values at $0.2T_C$ highlighted in bold: effective Mn concentration $[Mn]_{eff}$, approximate phosphorus concentration [P], lattice mismatch (lm), Curie temperature T_C and magnetic anisotropy coefficients[16]. V_{max} is the maximum velocity expected in the stationary regime from the 1D model (Eq. (1) and Ref. 3). $v_{max}(H_{max})$ is the maximum observed velocity. When 2 plateaus were observed, both values of maximum field/velocities are given.

of-plane anisotropy coefficient $K_\perp$=$\mu_0 M_s^2$/2-$K_{2\perp}$-$\frac{3}{2}K_{4//}$ and a uniaxial in-plane anisotropy coefficient K_0=$K_{2//}$-$K_{4//}$. The strained lattice mismatch (lm) is defined as $(a_\perp\text{-}a_{sub})/a_{sub}$, where $a_\perp$ is the strained lattice parameter of the film parallel to the growth axis and a_{sub} is the lattice parameter of the substrate. $[Mn]_{eff}$ is defined as the concentration of magnetically active Mn atoms.

Phosphorus alloying has been shown to be well suited to tune the strain and the magnetic properties of the layers, through their dependence on the valence band structure[15,17]. Decreasing the phosphorus concentration from $y \approx$3.4 to 0% at constant $[Mn]_{eff}$=3.7% increases the strained lattice mismatch from 0 to 6890 ppm. The strain-induced uniaxial out-of-plane anisotropy constant ($K_\perp$) consecutively increases, with the uniaxial in-plane anisotropy constant (K_0) remaining low. Rising $[Mn]_{eff}$ to 4.7% keeping y=0% further increases both in-plane and out-of-plane anisotropies (Table I). For all samples, the easy axis is expected from FMR to be along $[1\bar{1}0]$ at $T\geq$20 K and between -4° and -13° degrees away from [100] below.

Direct observation of the DW propagation was done by longitudinal Kerr microscopy using an LED source (λ=632nm), a high numerical aperture (0.4) objective and a deported aperture diaphragm[18]. The set-up probes the horizontal component of the magnetization (Kerr axis). Two external coils surrounding the cryostat provide a homogeneous horizontal field H_{ext} (minimum risetime 60μs). Inside the cryostat, a homemade set of micro-coils was designed to apply in-plane pulsed fields H_{pul} of up to 42 mT (risetime 100 ns). Contrary to most DW propagation studies relying on transport measurements[11,19], this set-up permits the simultaneous imaging of the propagating domains with a large field of view and application of short field pulses (see Ref. 16 for experimental details).

In order to establish the optimum field orientation for the dynamic study, hysteresis loops were first obtained from Kerr microscopy images under a static field H_{ext} applied at various angles. For $T \geq$ 20 K and $H_{ext}//[1\bar{1}0]$ (easy axis) and along the Kerr axis, we observed square cycles for all samples, with coercive fields $\mu_0 H_c$ roughly increasing with the strain-induced anisotropy $K_\perp$. At T=0.2T_c, $\mu_0 H_c$=0.9, 1.2 and 2 mT for resp. C3, B3, A3; $\mu_0 H_c$=2 mT for A4. For $H_{ext}//[100]$ and along the Kerr axis, the domains remained along $[1\bar{1}0]$. The resulting contrast was about $\cos(\pi/4)$ times weaker than for $H_{ext}//[1\bar{1}0]$, indicating that the magnetization within the domains remained aligned along the easy axis regardless of the field orientation. For the subsequent DWP study, the field was therefore aligned along the easy axis of the sample, as well as with the Kerr axis. This configuration led to the observation of 180° charged DWs, as reported previously[20,21]. The layers were kept unpatterned to understand how the complex in-plane anisotropy of the material interplays with its uniaxial anisotropy in field-induced DW dynamics.

The DW velocity is measured by applying several field pulses, and measuring the DW displacement on snapshots taken in zero field between consecutive pulses[16]. Domains expanded anisotropically, along the easy axis direction. Figs. 1b,c show DW velocity measurements done on samples with the weakest out-of-plane uniaxial anisotropies of the $[Mn]_{eff}$=3.7% series, B3 and C3. Once the DWs depin around the coercive field, the velocity at 20/30 K rises quasi-linearly towards a peak of 186 m s^{-1} for B3 and $\approx$ 100 m s^{-1} for C3. It then *decreases* by up to 36% of its peak value. The behavior at 60 K is similar but nucleations prevent the observation of the velocity decrease after the peak (see Table I for velocity values at 60 K).

In order to test the influence of the perpendicular uniaxial anisotropy on the maximum velocity, the DW velocities of samples A4 and A3 (of higher $K_\perp$) were then measured for similar temperatures. For H_{pul} just below the coercive field, very few domains nucleate and they adopt a wedge shape (Fig. 2b and Ref. 16) very reminiscent of the saw-tooth domains seen on in-plane magnetized Py[22] or Fe[23]. This profile efficiently reduces the magnetostatic energy cost of a 180° charged DW. Such a shape could not be observed as clearly on samples B3, C3 because of the great number of nucleations, due to the much weaker $K_\perp$. Once again, domains expanded very anisotropically along the easy axis. The $v(H)$ data are shown in Figs. 1a and 2a.

After depinning, the velocity first rises very steeply

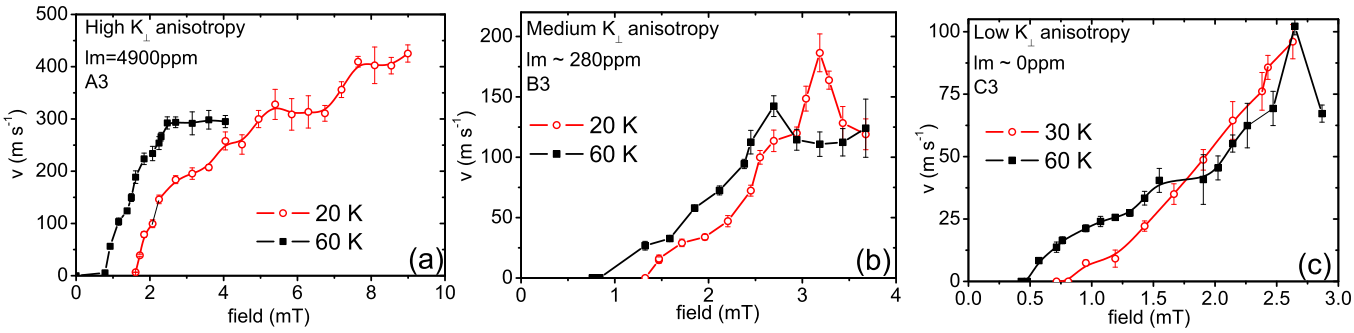

FIG. 1. Domain wall velocity versus applied field in the $[Mn]_{eff}$=3.7% series in order of decreasing lattice mismatch (slm) and uniaxial out-of-plane anisotropy. (a) A3, (b) B3, (c) C3. The lines are guides for the eyes.

with a mobility (dv/dH) that increases with temperature. For sample A3 at $T \approx 0.2T_C$, the velocity then plateaus at v_{max}=320 m s^{-1} above $\mu_0 H_{max}$=4.9 mT. At 7.6 mT, the velocity increases once again to reach a second plateau at 403 ms^{-1} (values of $\mu_0 H_{max}$ and v_{max} at 60 K in Table I). For sample A4 at $T \approx 0.2T_C$, there is only one clear velocity plateau of about 507 m s^{-1} reached at 7.8 mT ($\mu_0 H_{max}$, v_{max} at 60 and 85 K in Table I). The 85 K curve goes up to 481 m s^{-1} before nucleations prevent further measurement. The DW velocities measured on this sample are to our knowledge the highest observed to this day on any DMS. Moreover, they are close to - if not higher than - typical DW velocities encountered on unpatterned[6] and patterned[24] Permalloy. The observed velocities are moreover much higher than those measured on out-of-plane magnetized GaMnAs samples (field-[25] or current-induced[26] propagation) where they could only be measured up to a few tens of m s^{-1}. DW velocities measured on planar GaMnAs micron-wide stripes[11] were less than 0.1 m s^{-1}, very probably because the field was not applied along the easy axis which led to the formation of slower 90° domain walls.

Two main issues are raised up by the experiments presented above: the dependence of the maximum velocity on the magnetic anisotropy, and the different shapes of the $v(H)$ curves between samples A4, A3 on the one hand, and B3, C3 on the other hand. Although the thickness of the layer (about 5 times the exchange length) and lack of DW confinement make a genuine 1D-type DW propagation unlikely[25,27], this theory provides useful guidelines. In the case of simultaneous perpendicular and in-plane uniaxial anisotropies, it demonstrates the existence of a stationary solution for a propagating DW up to the Walker field $H_W = \alpha K_\perp / \mu_0 M_S$, with α the Gilbert damping constant and M_S the saturation magnetization. The maximum velocity in the stationary regime is then not necessarily the Walker velocity $V_W = \gamma \Delta_0 \mu_0 H_W / \alpha$ reached at Walker breakdown[3], but rather V_{max} reached at $H_{max} = 2H_W(1+\kappa)^{1/4} \frac{\sqrt{1+\kappa}-1}{\kappa} < H_W$:

$$V_{max} = 2V_W \frac{\sqrt{1+\kappa}-1}{\kappa} \qquad (1)$$

In these equations, $\kappa = K_\perp / K_0$ reflects the ratio of the two anisotropies[3] and $\Delta_0 = \sqrt{\frac{A_{exc}}{K_0}}$ is the static DW width with A_{exc} the exchange constant. This is completely equivalent to the case of weakly perpendicularly magnetized samples[18], for which the parameter equivalent to κ is $1/Q = \mu_0 M_s^2 / 2K_\perp$. For our samples, the static DW width is then calculated to lie around $\Delta_0 \approx 50$ nm, over 10 times wider than the DW width estimated experimentally in perpendicularly-magnetized GaMnAs(P) layers[7]. This estimated Δ_0 is of the order of the widths measured for near-180° DWs by high-resolution electron holography on 500 nm thick in-plane magnetized GaMnAs[12].

The resulting calculated $v(H)$ curve of ideally propagating DWs is shown in Fig. 3a for various values of K_0, $K_\perp$. The dependence of the maximum velocity on the magnetic anisotropies can be understood as follows for transverse DWs. When the field is applied along the easy axis, the DW magnetization starts precessing around it and comes out of the plane by an angle ϕ. The resulting magnetostatic charges created at the surfaces of the layer create a demagnetizing field H_{demag}: proportional to M_s in soft in-plane magnetized materials such as Py, or to the uniaxial anisotropy field $2K_\perp / \mu_0 M_s$ in the case of in-plane magnetization induced by magneto-crystalline anisotropy. It is the torque between H_{demag} and the DW's magnetization that propels the DW forward with a velocity proportionnal to H_{demag} and $\Delta(\phi)$. As the applied field increases, so does ϕ, resulting in the progressive shrinking of the DW width from its static value, becoming: $\Delta(\phi) = \frac{\Delta_0}{\sqrt{1+\kappa sin^2 \phi}}$. At small κ, this non-linearity is minor, and the mobility is linear up to Walker breakdown (κ=1 curve in Fig. 3a). As κ increases, the end of the stationary regime evolves into a broad plateau. Its amplitude rises with *increasing* out-of-plane anisotropy coefficient $K_\perp$ (through its effect on H_{demag}), but also with *decreasing* in-plane anisotropy as this will broaden the DW, and increase the velocity. The $1/\sqrt{K_0}$ dependence of the velocity is however weaker than the linear dependence on $K_\perp$. In the case

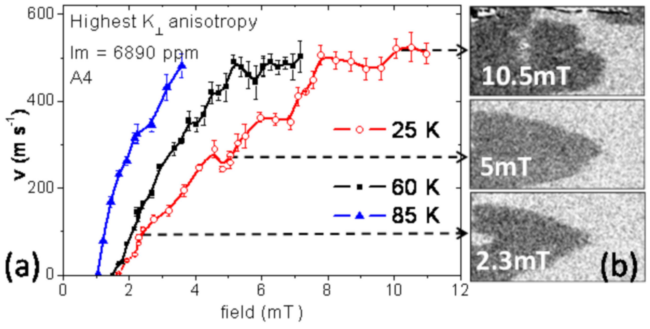

FIG. 2. (a) Domain wall velocity for the $[Mn]_{eff}$=4.7% sample at T=25, 60 and 85 K. (b) Modification of the domain profile with increasing field.

of $\kappa \gg 1$, the expression of the maximum velocity can in fact be simplified to $V^{\infty}_{max} \approx \frac{2\gamma}{M_s}\sqrt{A_{exc}K_{\perp}}$, evidencing once more the weaker influence of the uniaxial in-plane anisotropy on the maximum speed. In Permalloy nanowires, the magnetic anisotropy mainly results from the shape of the wire, and typical κ are close to 1. In our samples on the contrary, κ=20-200 (Table I).

In the framework of this model, and taking into account that the DWs depin at a finite field (very close to the coercive field) two different experimental scenarios can occur as shown schematically in Fig. 3b: the DW propagation can meet the intrinsic regime either before (dashed line) or after (dotted line) the Walker field. We attribute samples A3, A4 to the first category, and samples B3, C3 to the second one.

For samples with very low anisotropy fields (B3, C3), the Walker field is expected to be quite small, and the DW velocity meets directly the *precessional* regime (dotted line in Fig. 3b), at which point the velocity decreases with field. An upper boundary for the damping constant can then be estimated from $H_W=\alpha K_{\perp}/\mu_0 M_S$. Using the anisotropy coefficients determined by FMR and the experimental peak fields H_{max} at different temperatures (Table I) then yields α_{max}=0.02-0.04. This value is very much of the order found by variable-frequency FMR[28], but ten times smaller than the one estimated from the ratio of stationary and precessional mobilities (μ_{stat}, μ_{prec}) in out-of-plane magnetized GaMnAs[9]. Although this discrepancy has been pointed out before[29], it may also originate from an incorrect evaluation of μ_{stat} in these samples. Finally, calculating the field expected to give the maximum velocity at $T\approx 0.2T_c$ gives: $\mu_0 H_{max}$=1.2 mT (1.5 mT) for sample C3 (B3). These are barely above their coercive fields $\mu_0 H_c$=0.9 mT (1.2 mT), which explains why the high velocity plateau is not seen at all.

For samples with higher anisotropy fields (A3, A4), it is the *stationary* regime that is reached after depinning (dashed line in Fig. 3b). This occurs at exceptionally high speeds ($\approx$ 150 m s^{-1} for A3 and $\approx$ 300 m s^{-1} for A4) which contrasts strongly with the claims of Ref. 11 of a stationary regime reached by 8.10^{-2} m s^{-1}. The expected saturation velocities calculated from Eq. (1) at $T\approx 0.2T_c$ from the 1D model are indicated in Table I for samples A3 and A4. For this calculation, the exchange constant was taken as 3.10^{-13} J m^{-1} for $[Mn]_{eff}$=4.7% (sample A4) and as 10^{-13} J m^{-1} for $[Mn]_{eff}$=3.7% (sample A3), as estimated on perpendicularly magnetized samples of similar manganese content[7]. The experimentally determined velocities follow the predicted trend of increasing V_{max} with perpendicular anisotropy $K_{\perp}$, as well as the weaker influence of the in-plane anisotropies (Table I). However, the observed maximum velocities are underestimated by a factor of about 1.5, and the velocity plateaus are unexpected within this model. As evidenced repeatedly in both simulations[3] and experiments[30], an abrupt change in velocity often results from a modification of the nature of the DW. A modification of the domain profile can indeed be seen on the domain images of samples A3 and A4 (Fig. 2b). The domain gradually loses its sawtooth shape and smoothens out with increasing field, or more exactly divides up into sawtooths of shorter period. These DW transformations could be the reason for the plateaus observed for samples A3 and A4. To summarize, the 1D model provides gives good qualitative trends, but underestimates the observed velocities, possibly due to a transformation of the DW profile.

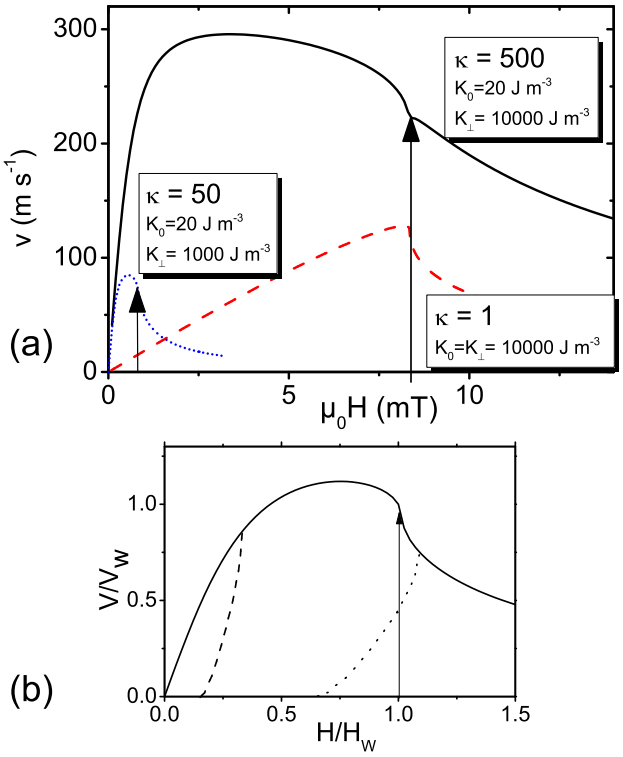

FIG. 3. Computed 1D model $v(H)$ curves with the vertical arrows indicating the position of the Walker field. (a) Varying in-plane (K_0) and out-of-plane ($K_{\perp}$) anisotropies without pinning (following Ref. 3 with α=0.03, A_{exc}=10^{-13} J m^{-1}, M_s=36 kA m^{-1}). (b) Possible modifications to the $v(H)$ curve when pinning is taken into account. The DW velocity may rejoin the intrinsic regime before Walker breakdown (dashed line) or afterwards (dotted line).

This work gives clear guidelines for designing high speed DW based devices. In particular, the largest DW velocities are found for 180° charged DWs propagating along the easy axis, with layers exhibiting the largest out-of-plane anisotropy and a weak in-plane anisotropy, which corresponds to a large DW width. Lateral confinement of the DWs through nanostructuration of the layer is expected to have a further impact on the maximum velocity since it will affect the uniaxial in-plane anisotropy, as already shown in GaMnAs[31]. In light of our results, this additional parameter would open a wide range of possibilities to control the DW dynamics in field- or current- driven DW motion experiments.

We acknowledge C. Doré and S. Majrab for technical assistance. This work was performed in the framework of the MANGAS project (ANR 2010-BLANC-0424-02).

[1] S. S. P. Parkin, M. Hayashi, and L. Thomas, *Science* **320**, 190 (2008).
[2] H. T. Zeng, D. Read, L. OBrien, J. Sampaio, E. R. Lewis, D. Petit, and R. P. Cowburn, *Appl. Phys. Lett.* **96**, 262510 (2010).
[3] A. Thiaville and Y. Nakatani, Spin Dynamics in Confined Magnetic Structures III, p. 183, Springer, New York, 2006.
[4] R. Moriya, M. Hayashi, L. Thomas, C. Rettner, and S. S. P. Parkin, *Appl. Phys. Lett.* **97**, 142506 (2010).
[5] K. Yamada, J.-P. Jamet, Y. Nakatani, A. Mougin, A. Thiaville, T. Ono, and J. Ferré, *Appl. Phys. Expr.* **4**, 113001 (2011).
[6] S. Middelhoek, *IBM J. Res. Dev.* **10**, 351 (1966).
[7] S. Haghgoo, M. Cubukcu, H. von Bardeleben, L. Thevenard, A. Lemaître, and C. Gourdon, *Phys. Rev. B* **82**, 041301(R) (2010).
[8] L. Thevenard, L. Largeau, O. Mauguin, A. Lemaître, K. Khazen, and H. von Bardeleben, *Phys. Rev. B* **75**, 195218 (2007).
[9] A. Dourlat, V. Jeudy, A. Lemaître, and C. Gourdon, *Phys. Rev. B* **78**, 161303 (2008).
[10] L. Herrera Diez, J. Honolka, K. Kern, E. Placidi, F. Arciprete, A. W. Rushforth, R. Campion, and B. Gallagher, *Phys. Rev. B* **81**, 094412 (2010).
[11] H. Tang, R. Kawakami, D. Awschalom, and M. Roukes, *Phys. Rev. B* **74**, 041310(R) (2006).
[12] A. Sugawara, H. Kasai, a. Tonomura, P. Brown, R. Campion, K. Edmonds, B. Gallagher, J. Zemen, and T. Jungwirth, *Phys. Rev. Lett.* **100**, 1 (2008).
[13] N. L. Schryer and L. R. Walker, *J. Appl. Phys.* **45**, 5406 (1974).
[14] A. Malozemoff and J. Slonczewski, *Phys. Rev. Lett.* **29**, 952 (1972).
[15] M. Cubukcu, H. J. von Bardeleben, K. Khazen, J. L. Cantin, O. Mauguin, L. Largeau, and A. Lemaître, *Phys. Rev. B* **81**, 41202 (2010).
[16] *Please refer to Supplemental Materials for details.*
[17] A. Lemaître, A. Miard, L. Travers, O. Mauguin, L. Largeau, C. Gourdon, V. Jeudy, M. Tran, and J. George, *Appl. Phys. Lett.* **93**, 21123 (2008).
[18] A. Hubert and R. Schäfer, *Magnetic domains*, Berlin, Springer edition, 2000.
[19] S. Corodeanu, H. Chiriac, and T.-A. Ovari, *Rev. Sci. Instr.* **82**, 094701 (2011).
[20] U. Welp, V. K. Vlasko-Vlasov, X. Liu, J. K. Furdyna, and T. Wojtowicz, *Phys. Rev. Lett.* **90**, 167206 (2003).
[21] J. Honolka, L. Herrera Diez, R. K. Kremer, K. Kern, E. Placidi, and F. Arciprete, *New J. Phys.* **12**, 093022 (2010).
[22] L. Finzi and J. Hartman, *IEEE Trans. Mag.* **4**, 662 (1968).
[23] W. Lee, B.-C. Choi, Y. Xu, and J. Bland, *Phys. Rev. B* **60**, 10216 (1999).
[24] M. Hayashi, L. Thomas, C. Rettner, R. Moriya, and S. S. P. Parkin, *Nat. Phys.* **3**, 21 (2006).
[25] L. Thevenard, C. Gourdon, S. Haghgoo, J. P. Adam, H. von Bardeleben, A. Lemaître, W. Schoch, and A. Thiaville, *Phys. Rev. B* **83**, 245211 (2011).
[26] J. P. Adam, N. Vernier, J. Ferré, A. Thiaville, V. Jeudy, A. Lemaître, L. Thevenard, and G. Faini, *Phys. Rev. B* **80**, 193204 (2009).
[27] C. Zinoni, A. Vanhaverbeke, P. Eib, G. Salis, and R. Allenspach, *Phys. Rev. Lett.* **107**, 207204 (2011).
[28] K. Khazen, H. von Bardeleben, M. Cubukcu, J. Cantin, V. Novak, K. Olejnik, M. Cukr, L. Thevenard, and A. Lemaître, *Phys. Rev. B* **78**, 1 (2008).
[29] G. Vella-Coleiro, *Appl. Phys. Lett.* **21**, 36 (1972).
[30] M. Kläui, P.-O. Jubert, R. Allenspach, A. Bischof, J. Bland, G. Faini, U. Rüdiger, C. Vaz, L. Vila, and C. Vouille, *Phys. Rev. Lett.* **95**, 026601 (2005).
[31] J. Wenisch, C. Gould, L. Ebel, J. Storz, K. Pappert, M. J. Schmidt, C. Kumpf, G. Schmidt, K. Brunner, and L. W. Molenkamp, *Phys. Rev. Lett.* **99** (2007).